FOREX Publication
Open Access | Rapid and quality publishing

International Journal of
Electrical and Electronics Research (IJEER)
Research Article | Volume 12, Issue 4 | Pages 1522-1530 | e-ISSN: 2347-470X

Harmonic Analysis of Stator Current for Grid Connected Five Phase Open End Winding Squirrel Cage Induction Generator Using Indirect Rotor Field Oriented Control Technique with Three Level Rectifier

Swetha Kannepally[1], Ch. Murali[2], Mantri Srinivasarao[3], S Srikanth[4], and Adabala Ramakrishna[5]

[1]*Assistant Professor, Department of EEE, S.R.K.R Engineering College, Bhimavaram, Andhra Pradesh, India; swet07@gmail.com*
[2]*Assistant Professor, Department of EEE, S.R.K.R Engineering College, Bhimavaram, Andhra Pradesh, India; chmvsraju@gmail.com*
[3]*Professor, Department of EEE, Bonam Venkata Chalamayya Engineering College, Odalarevu, Andhra Pradesh, India; msr.bvce@bvcgroup.in*
[4]*Professor, Department of EEE, Bonam Venkata Chalamayya Engineering College, Odalarevu, Andhra Pradesh, India; srikanth.bvce@bvcgroup.in*
[5]*Associate Professor, Department of EEE, Bonam Venkata Chalamayya Engineering College, Odalarevu, Andhra Pradesh, India; arkrishna.bvce@bvcgroup.in*

***Correspondence:** Swetha Kannepally; *swet07@gmail.com*

ABSTRACT- The rising need for renewable energy sources requires the optimization of power generation systems, especially in wind energy applications. The five-phase open end winding induction generator offers benefits such as less torque ripple and improved fault tolerance relative to conventional three-phase systems. The Indirect Rotor Field Oriented Control Technique for five phase open end winding squirrel cage induction generator separates the control of electromagnetic torque and rotor flux, allowing for accurate regulation of generator output in fluctuating wind conditions. The control technique utilizes a three-level rectifier to enhance power conversion efficiency, resulting in a more stable voltage output during various wind speeds and diminished harmonic distortion. This paper examines the performance of application of Indirect Rotor Field Oriented Control Technique for Five Phase Open End Winding Squirrel Cage Induction Generator in wind energy systems, coupled with a three-level rectifier. The simulation findings illustrate the harmonic distortion of stator current with three level rectifier is better than two level rectifiers for Five Phase Open End Winding Squirrel Cage Induction Generator during step change in wind speeds.

Keywords: SCIG, WECS, IFOC, MLR, THD, FPOEWSCIG.

ARTICLE INFORMATION

Author(s): Swetha Kannepally, Ch. Murali, Mantri Srinivasarao, S Srikanth, and Adabala Ramakrishna;

Received: 05/10/2024; **Accepted**: 10/12/2024; **Published**: 30/12/2024;
e-ISSN: 2347-470X;
Paper Id: IJEER 0510-04;
Citation: 10.37391/ijeer.120449
Webpage-link:
https://ijeer.forexjournal.co.in/archive/volume-12/ijeer-120449.html

Publisher's Note: FOREX Publication stays neutral with regard to Jurisdictional claims in Published maps and institutional affiliations.

1. INTRODUCTION

In recent years, wind power has quickly become a leading renewable energy source. The need for renewable energy sources is growing in response to rising international alarm over climate change and environmental deterioration. A promising substitute for fossil fuels, wind power, which is generated from the kinetic energy of the wind, helps to diversify energy sources and reduce emissions of greenhouse gases [1]. A vital part of the worldwide movement to a low-carbon economy [2], wind power does not directly release carbon dioxide (CO_2) or any other dangerous pollutants, unlike traditional energy sources like coal, oil, or natural gas.

The development of several turbine technologies to efficiently harness wind power has made wind energy an essential component of renewable energy initiatives worldwide. Using a squirrel cage induction generator (SCIG), the Type-4 wind turbine has become one of the most well-known and efficient technologies in contemporary wind energy systems. Complete regulation of active and reactive power [7] is achieved by use of a back-to-back converter, which is inherent to the Type-4 wind turbine as a fully-converter-based system. Type-4 wind turbines benefit greatly from grid integration and operational flexibility to this configuration, which allows them to operate over a wide range of wind speeds. Type-4 wind turbines equipped with SCIGs have numerous benefits, but they also come with certain problems that need fixing. The power electronics add unnecessary complexity and expense to the system, which is its biggest downside.

Open-end winding squirrel cage induction generators have garnered considerable interest in wind energy conversion

FOREX Publication
Open Access | Rapid and quality publishing
International Journal of Electrical and Electronics Research (IJEER)
Research Article | Volume 12, Issue 4 | Pages 1522-1530 | e-ISSN: 2347-470X

systems owing to its distinctive design and operating benefits. With the increasing global demand for renewable energy sources, it is essential to utilize effective technology for harnessing wind energy. The open-end winding architecture of the SCIG provides increased flexibility and adaptability, rendering it a crucial element in contemporary wind turbine designs [10]. A principal advantage of open-end winding SCIG is its capacity to provide both generator and motor functions. This dual functionality enables wind turbines to work efficiently under diverse wind speeds and load situations. The generator can seamlessly transition to motor mode in low wind circumstances, allowing the turbine to sustain peak performance and energy extraction [11].

The wind energy conversion systems (WECS) have taken notice of multiphase machines because they outperform conventional three-phase machines in terms of performance, reliability, and fault tolerance. Offshore and large-scale wind farms [13] have been early adopters of multiphase machines due to the increasing need for high-power wind turbines and more efficient energy conversion. Machines with five-, six-, or even nine-phase designs are a promising technology for wind energy systems of the future because of the many benefits they provide in terms of operating flexibility, power density, and system durability.

The enhanced fault tolerance of multiphase machines is a major advantage in WECS. If there is a problem with any one phase in a traditional three-phase system, the wind turbine will stop working altogether. Because of the high maintenance costs and limited accessibility to offshore wind farms, this inherent fault-tolerant capability is particularly critical. A more available wind energy system [14] with less downtime is possible with partial operation maintenance during faults.

Multiphase machines also have the benefit of a higher power density. In order to achieve the same power output with less per-phase current, multiphase machines spread the current across many phases. This results in improved thermal management and decreased copper losses [15]. Because of the need for dynamic control to optimize energy capture in wind energy systems, this is especially advantageous in these contexts. Further, multiphase machines have the ability to run at lower harmonics, which improves the quality of the power that is injected into the grid and decreases electromagnetic noise.

Indirect Field Oriented Control (IFOC) has become an essential method for the effective regulation of squirrel cage induction generators (SCIG) in wind energy conversion systems (WECS). With the escalating demand for renewable energy sources, enhancing the efficiency of wind turbines is becoming progressively vital. IFOC provides substantial benefits for dynamic responsiveness, control accuracy, and energy efficiency, rendering it an optimal solution for SCIGs employed in variable-speed wind turbines [17]. This technology optimizes the generator's performance, facilitating enhanced energy extraction from variable wind conditions. One of the principal advantages of IFOC is its capacity to decouple the regulation of torque and flux in the SCIG. By independently addressing the machine's magnetic field and torque components, IFOC facilitates enhanced control over the generator's performance. This decoupling is especially beneficial in wind energy systems, because fluctuating wind speeds require swift modifications in generator performance [18]. The accurate regulation of torque and flux facilitates smoother operation and enhanced efficiency, essential for optimizing energy extraction from wind resources. Moreover, IFOC enables SCIGs to function at varying speeds, hence ensuring optimal performance under diverse wind conditions. In contrast to conventional control systems that necessitate the generator to function at a constant speed, IFOC allows SCIGs to modify their rotational speed in accordance with varying wind velocities. This capacity promotes energy efficiency and improves the overall reliability of the wind turbine system [19].

Based on Multilevel inverters concept Multilevel rectifiers (MLR) have evolved as a revolutionary technique in the regulation of squirrel cage induction generators (SCIG) in wind energy conversion systems (WECS). With the escalating demand for renewable energy sources, the necessity for efficient, reliable, and high-performance power conversion systems intensifies. MLR mitigate these issues by offering superior voltage regulation, less harmonic distortion, and higher overall system efficiency [24]. This characteristic renders them especially appropriate for wind energy applications, where variable speed operation and grid integration are crucial.

A key advantage of employing MLRs in WECS is their capacity to produce high-quality output voltage waveforms. Conventional two-level rectifiers frequently generate considerable harmonic distortion, which can negatively impact the efficiency of induction generators and result in heightened losses [25]. Conversely, MLIs employ various voltage levels to generate a more refined output waveform, leading to less total harmonic distortion (THD). This enhancement not only increases the efficiency of the SCIG but also improves electricity quality in grid [26].

FOREX Publication
Open Access | Rapid and quality publishing
International Journal of Electrical and Electronics Research (IJEER)
Research Article | Volume 12, Issue 4 | Pages 1522-1530 | e-ISSN: 2347-470X

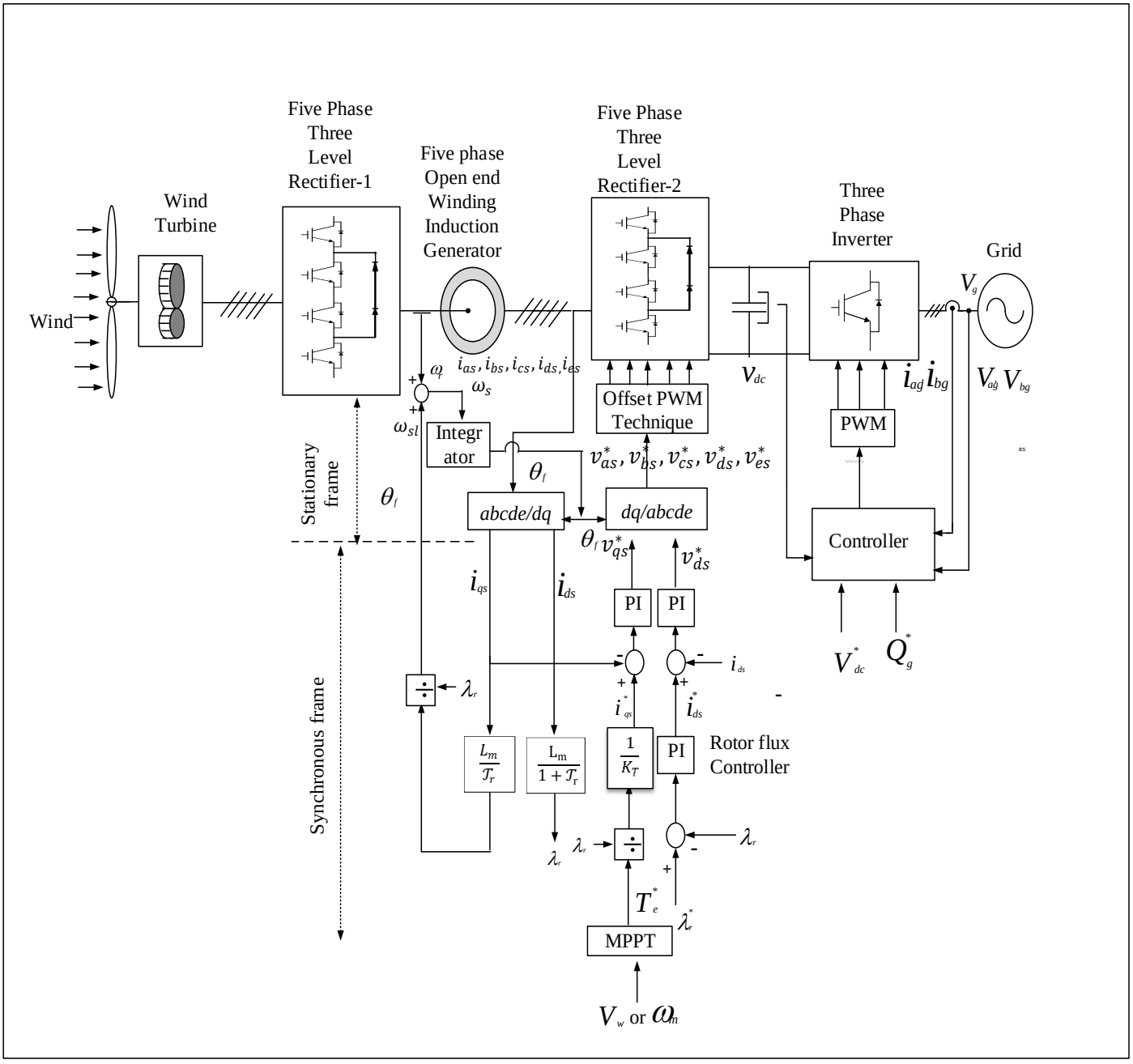

Figure 1. Schematic Diagram of Indirect Rotor Field Oriented Vector Control for Five-Phase Open End Winding Squirrel Cage Induction Generator with Three Level Rectifier in Wind Energy System

2. MATHEMATICAL MODEL OF WIND TURBINE

Incorporating the concept of Cp (Coefficient of Performance) enables the formulation of a precise mathematical model for the wind turbine. The potential energy of air moving through a wind turbine with a surface area of A and a speed of V m/sec can be expressed as [27]

$$P_w = 0.5\rho AV^3 \quad (1)$$

Where P_w : wind power
A: area swept by blades in m^2
V: speed of the wind m/sec
ρ: air density - kg/m^3

"The power coefficient of the turbine, denoted as *Cp* (λ, β), demonstrated by the pitch angle (β) & the tip-speed ratio (λ).

The article describes the wind energy captured by the wind turbine."

$$\lambda = \frac{\omega_t R}{V} \quad (2)$$

ω_t The turbine speed is measured in radians/second.
R -wind turbine's radius is measured in meters.

FOREX Publication
Open Access | Rapid and quality publishing
International Journal of Electrical and Electronics Research (IJEER)
Research Article | Volume 12, Issue 4 | Pages 1522-1530 | e-ISSN: 2347-470X

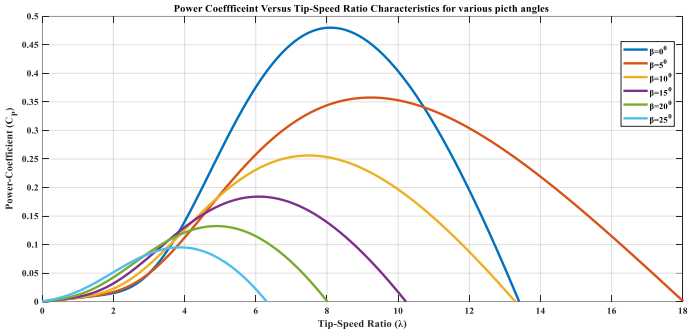

Figure 2. Power coefficient characteristic for different pitch angles

Figure 2 shows that wind turbines have a maximum power co-efficient of 0.49 at pitch angle $\beta = 0^0$. *Equation (1)* shows that the mechanical power of the wind turbine is proportional to the cube of the wind velocity. From cut-in wind speed (6 m/sec) to rated wind speed (13 m/sec), pitch angle is kept at 0^0 to maximize mechanical power from the wind. When wind speed exceeds the rated value of 13 m/sec, the mechanical power of the wind turbine increases proportionally to the cube of wind velocity. To reduce wind turbine mechanical power, the pitch angle (β) is gradually increased.

Wind-powered machinery is provided with mechanical power by

$$P_m = 0.5\rho A V^3 C_P(\lambda, \beta) \quad (3)$$

Where, P_m : Mechanical power (Watts)
C_P : coefficient power
β : Pitch angle of blade in degrees

$$C_P = 0.517\left(\frac{116}{\lambda_i} - 0.4\beta - 5\right)e^{-\frac{21}{\lambda_i}} + 0.068\lambda$$

$$\frac{1}{\lambda_i} = \frac{1}{\lambda + 0.08\beta} - \frac{0.035}{\beta^3 + 1}$$

Mechanical power parameters at different wind speeds range from 6 to 13 meters per second are shown in *fig.3*. The wind turbine has a mechanical power rating of 2.0 Mega Watts (MW) at a wind speed of 12m/sec.

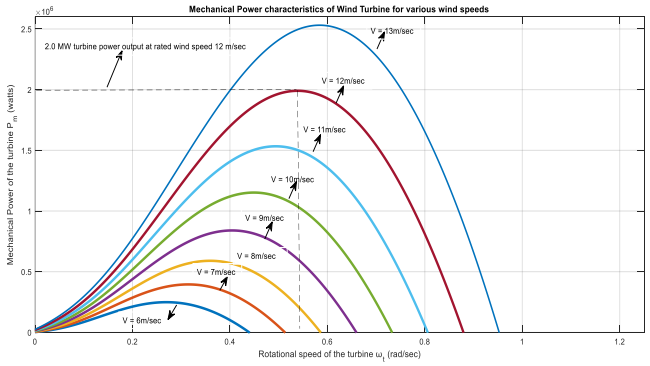

Figure 3. Mechanical Power Characteristics for different wind speeds

Figure 3 illustrates the mechanical power characteristics of the wind turbine with wind speeds ranging from 6 m/s to 13 m/s. The wind turbine generates a maximum mechanical power of 2.0 Mega Watts (MW) at a wind speed of 12 m/sec. When the mechanical power of a wind turbine surpasses its rated mechanical power due to an increase in wind speed, it should be regulated to the rated value by altering the pitch angle β. The mechanical power produced by the wind turbine at different wind speeds, as seen in *fig. 3*, is supplied to the five-phase squirrel cage induction generator to produce electrical power. The reference torque is derived from mechanical power and is regarded as a negative value.

3. MATHEMATICAL MODEL OF FIVE PHASE OPEN END WINDING SQUIRREL CAGE INDUCTION GENERATOR

The dq- axis voltages and fluxes obtained are to be expressed in phasor form for applying proposed control techniques. Using *equations (4 to 7)* dynamic equations of an FPOEWAG expressed [28] in terms of d-q model:

On Stator side voltage equations are

$$v_{ds} = i_{ds}r_s + p\lambda_{ds} - \omega_s\lambda_{qs} \quad (4)$$

$$v_{qs} = i_{qs}r_s + p\lambda_{qs} + \omega_s\lambda_{ds} \quad (5)$$

On Rotor side voltage equations are

$$v_{dr} = i_{dr}r_r + p\lambda_{dr} - (\omega_s - \omega_r)\lambda_{qr} \quad (6)$$

$$v_{qr} = i_{qr}r_r + p\lambda_{qr} + (\omega_s - \omega_r)\lambda_{dr} \quad (7)$$

v_{dq}^s : d-q axis stator voltage in volts

v_{dq}^r : d-q axis stator voltage in volts

i_{dq}^s : d-q axis stator current in Amperes

i_{dq}^r : d-q axis stator current in Amperes

λ_{dq}^s : d-q axis stator flux-linkage in webers

λ_{dq}^r : d-q axis rotor flux-linkage in webers

4. MODELLING OF FIVE PHASE THREE LEVEL RECTIFIER

$S_1, S_{11}, S_2, S_{22} S_3, S_{33} S_4, S_{44}, S_5, S_{55}$ are top switches and belongs to positive polarity for five-phase rectifier. $S_1', S_{11}', S_2', S_{22}', S_3', S_{33}', S_4', S_{44}', S_5', S_{55}'$ are bottom switches and belongs to negative polarity for five-phase rectifier If top switch in *fig.4* is "ON," bottom switch should be "OFF," and vice-versa for two switches on the same leg of the power source.

FOREX Publication
Open Access | Rapid and quality publishing
International Journal of Electrical and Electronics Research (IJEER)
Research Article | Volume 12, Issue 4 | Pages 1522-1530 | e-ISSN: 2347-470X

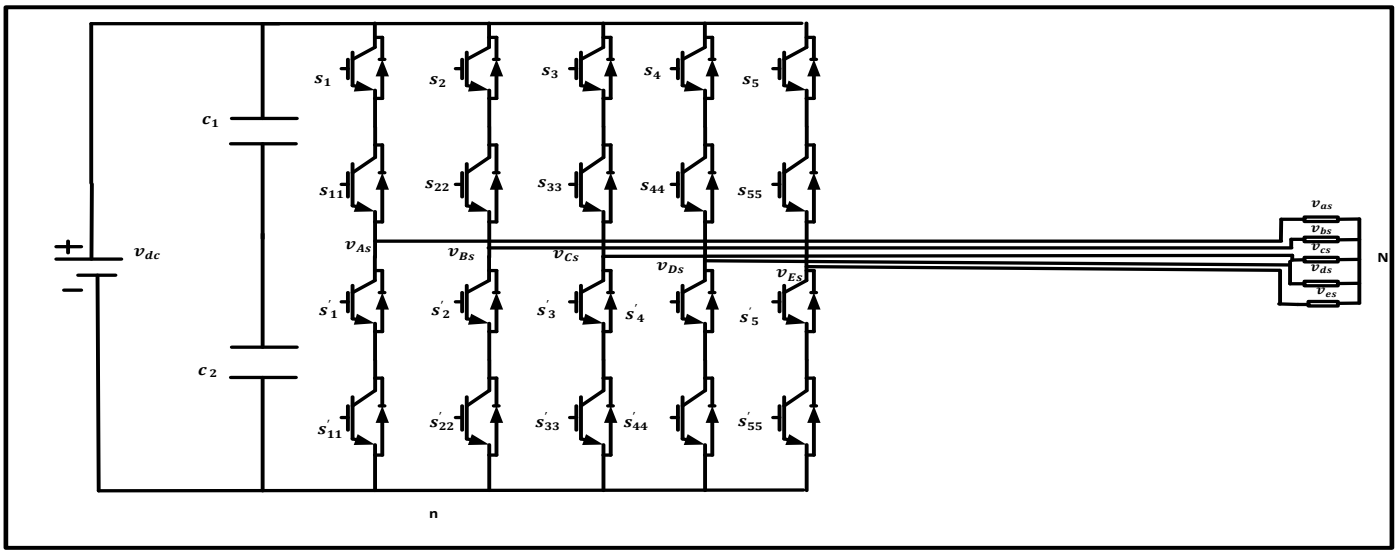

Figure 4. Schematic Diagram of Five Phase Three Level Rectifier

Relationship between pole voltages and phase-to-neutral load voltage is [28]:

$$\left.\begin{aligned} V_{AS}(t) &= V_{aS}(t) + V_{nN}(t) \\ V_{BS}(t) &= V_{bS}(t) + V_{nN}(t) \\ V_{CS}(t) &= V_{cS}(t) + V_{nN}(t) \\ V_{DS}(t) &= V_{dS}(t) + V_{nN}(t) \\ V_{ES}(t) &= V_{eS}(t) + V_{nN}(t) \end{aligned}\right\} \quad (8)$$

Where

$V_{AS}(t), V_{BS}(t), V_{CS}(t), V_{DS}(t), V_{ES}(t)$ are pole voltages for five-Phase Rectifier

$V_{aS}(t), V_{bS}(t), V_{cS}(t), V_{dS}(t), V_{eS}(t)$ are load voltages for five-Phase Rectifier and

V_{nN} – difference between star point *n* for load and negative rail of DC bus N known as common mode voltage.

$$V_{nN}(t) = 1/5((V_{AS}(t) + V_{BS}(t) + V_{CS}(t) + V_{DS}(t) + V_{ES}(t))$$

Substituting $V_{nN}(t)$ into $V_{AS}(t)$ equation (3.44) results into

$$\left.\begin{aligned} V_{aS}(t) &= \tfrac{4}{5}V_{AS}(t) - 1/5(V_{BS}(t) + V_{CS}(t) + V_{DS}(t) + V_{ES}(t)) \\ V_{bS}(t) &= \tfrac{4}{5}V_{BS}(t) - 1/5(V_{AS}(t) + V_{CS}(t) + V_{DS}(t) + V_{ES}(t)) \\ V_{cS}(t) &= \tfrac{4}{5}V_{CS}(t) - 1/5(V_{AS}(t) + V_{BS}(t) + V_{DS}(t) + V_{ES}(t)) \\ V_{dS}(t) &= \tfrac{4}{5}V_{DS}(t) - 1/5(V_{AS}(t) + V_{BS}(t) + V_{CS}(t) + V_{ES}(t)) \\ V_{eS}(t) &= \tfrac{4}{5}V_{ES}(t) - 1/5(V_{AS}(t) + V_{BS}(t) + V_{CS}(t) + V_{DS}(t)) \end{aligned}\right\} \quad (9)$$

The resultant mathematical *equations (8 and 9)* are used to control five phase two level rectifiers for grid connected FPOESCIG. From the literature it is inferred that five phase two level rectifiers have limitations of increased losses and overall system efficiency reduction. To overcome this and also to reduce THD five phase three level rectifiers are used.

5. IFOC OF FIVE-PHASE OPEN-END WINDING SCIG

The open-end winding base FPOEWSCIG DFOC methods include rotor flux orientation, air gap flux, and stator flux. In contrast to the direct field-oriented method, the optimal strategy is rotor flux orientation. The two components of the squirrel cage induction generator's stator current space vector are i-$_{ds}$ and i-$_{qs}$. In rotor flux, orientation i_{ds} is rotor flux-producing component and i_{qs} is a torque-producing component.

The DFOC strategies for an open-end winding FPOEWSCIG are rotor flux orientation, stator flux, & air gap flux. The direct field-oriented method is not as effective as the rotor flux orientation method. There are two parts to the stator current space vector of a FPOEWSCIG: i_{ds} and i_{qs}. Rotor flux includes orientation i_{ds} as a component that produces rotor flux and i_{qs} as a component that produces torque [27].

This equation could be applied to determine the IFOC rotor flux angle from *fig. 1*.

$$\theta_f = \int \omega_r + \omega_{sl}\, dt \quad (10)$$

The rotor speed measured from the generator is denoted as ω_r, while the slip frequency is determined and represented as ω_{sl}. in rad/sec

Where ω_{sl} is computed slip frequency and ω_r is the observed rotor speed from the generator.

The equation describing the rotor space vector in the generator

FOREX Publication
Open Access | Rapid and quality publishing
International Journal of Electrical and Electronics Research (IJEER)
Research Article | Volume 12, Issue 4 | Pages 1522-1530 | e-ISSN: 2347-470X

framework can be used to calculate the slip frequency ω_{sl}.

$$\overrightarrow{v_r} = \overrightarrow{\imath_r}\mathrm{R}_r + p\overrightarrow{\phi_r} + j\omega_{sl}\overrightarrow{\phi_r} \quad (11)$$

From equation [11] equating rotor voltage $\overrightarrow{v_r} = 0$ and calculating $p\overrightarrow{\phi_r}$

Based on the formula [11] which states the rotor voltage $\overrightarrow{v_r} = 0$, and doing the math to determine $p\overrightarrow{\phi_r}$

$$p\overrightarrow{\phi_r} = -\overrightarrow{\imath_r}\mathrm{R}_r - j\omega_{sl}\overrightarrow{\phi_r} \quad (12)$$

In general

$$\overrightarrow{\phi_r} = L_r\overrightarrow{\imath_r} + L_m\overrightarrow{\imath_s} \quad (13)$$

From equation [13] rotor current can be

$$\overrightarrow{\imath_r} = \frac{1}{L_r}\left(\overrightarrow{\phi_r} - L_m\overrightarrow{\imath_s}\right)$$

Substituting the rotor current into *equation (12)* Yields

$$p\overrightarrow{\phi_r} = \frac{R_r}{L_r}\left(\overrightarrow{\phi_r} - L_m\overrightarrow{\imath_s}\right) - j\omega_{sl}\overrightarrow{\phi_r} \quad (14)$$

From which

$$\overrightarrow{\phi_r} = \left(1 + \tau_r\left(p + j\omega_{sl}\right)\right) = L_m\overrightarrow{\imath_s} \quad (15)$$

Rotor flux reference ($\emptyset_r^*$is typically set at 1.803webers, whereas actual flux can be determined from the actual rotor flux could be retrieved by setting the rotor flux reference $\emptyset_r^*$to its rated value, which is typically 1.803 webers.

From equation [15]

$$\phi_r(1 + p\tau_r) = L_m i_{ds} \quad (16)$$

Equation [17] describes the electromagnetic torque of an induction generator, which is defined as the multiplication of the rotor flux as well as the stator currents.

$$T_e = \frac{5}{2}PL_m\left(i_{qs}\phi_{dr} - i_{ds}\phi_{qr}\right) \quad (17)$$

The properties of the synchronous reference frame are utilized for calculating the rotor element's flux applying formula [17].

$$\phi_{qr} = 0$$

$$\phi_{dr} = \phi_r$$

Substituting in *equation (17)* then

$$T_e = \frac{5}{2}PL_m(i_{qs}\phi_r) \quad (18)$$

If ϕ_r remains constant while the generator is operating, the electromagnetic equation T_e is directly proportional to i_{qs}, as shown in equation [18].

$$T_e = K_T i_{qs}$$

$$K_T = \frac{5}{2}PL_m\phi_r$$

The term K_T is called as torque constant.

T_m (Mechanical torque) is produced by the wind turbine throughout cut-in speed & rated wind speeds directly proportional to T_e^*. i_{qs}^* q-axis reference current is acquired utilizing the *equation (18)*.

It is assumed that the mechanical torque T_m, which is produced by wind turbines at cut-in speed & rated wind speeds, directly proportional to T_e^*. To get the i_{qs}^* q-axis reference current, the following *equation (19)* is used:

$$i_{qs}^* = \frac{T_e^*}{(K_T\tau_r)} \quad (19)$$

Feedback d-q axis currents in *fig.1* $i_{ds}$and i_{qs} are measured employing current sensors followed by being compared to their respective reference currents. i_{ds}^* and i_{qs}^*. Errors are transmitted to the respective PI-Controllers to create stator voltage references $v^*{}_{ds}$ & $v^*{}_{qs}$. The $v^*{}_{ds}$ and $v^*{}_{qs}$ could be provided to a 5-phase offset additional PWM block to produce the required switching signals for a 5-phase rectifier. The $v_{as}^*, v_{bs}^*, v_{cs}^*, v_{ds}^*, v_{es}^*$ are the five-phase offset addition block will produce voltages.The currents i_{ds}^* and i_{qs}^*., which represent the feedback of d-q axis currents in *figure1*, are measured by current sensors and subsequently compared to their corresponding reference currents. To create stator voltage references $v^*{}_{ds}$ & $v^*{}_{qs}$., the errors are communicated to the relevant PI-Controllers. The 5-phase offset addition PWM block could be employed to create the switching signals needed for the five-phase rectifier by feeding the $v^*{}_{ds}$ and $v^*{}_{qs}$ signals.

Equation (20) is used to determine V_offset, and the five-phase offset addition block will produce voltages $v_{as}^*, v_{bs}^*, v_{cs}^*, v_{ds}^*, v_{es}^*$.

$$V_{offset} = -\frac{V_{max}+V_{min}}{2} \quad (20)$$

6. TESTING OF FIVE PHASE OPEN END WINDING INDUCTION GENERATOR WITH IFOC TECHNIQUE WITH THREE LEVEL RECTIFIER USING MATLAB/SIMULINK

Wind speed 12 m/sec is considered as 1 p.u and the step changes are taken from 0.6 p.u to 1 p.u. The proposed mathematical model of IFOC with three level rectifiers for five phase open end winding induction generator is tested at step change in wind speeds at 7.2 m/sec, 9.6 m/sec, and 12 m/sec in MATLAB/ SIMULINK Environment.

In order to compare the performance of proposed control IFOC technique for five phase open end winding induction with three level rectifier the simulation results of IFOC technique with two level rectifiers for the proposed generator are also presented.

FOREX Publication
Open Access | Rapid and quality publishing
International Journal of Electrical and Electronics Research (IJEER)
Research Article | Volume 12, Issue 4 | Pages 1522-1530 | e-ISSN: 2347-470X

The simulation results for five phase stator voltages for three level rectifier-1, three level rectifier-2, resultant voltages of stator, stator flux, rotor flux, d and q –axis of stator currents, five phase stator currents, electromagnetic torque, are presented.

7. SIMULATION RESULTS OF FIVE PHASE OPEN END WINDING SQUIRREL CAGE INDUCTION GENERATOR USING IFOC TECHNIQUE WITH TWO LEVEL RECTIFIERS

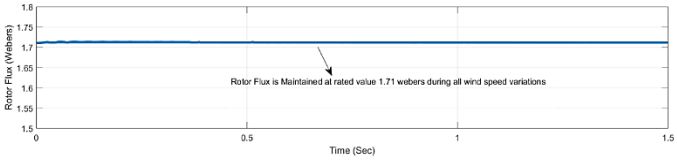

Figure 5. Rotor Flux of Five Phase Open End Winding Squirrel Cage Induction Generator

From *figure 5*, it is observed that rotor flux is maintained at its rated value 1.71 webers during all wind speed variations.

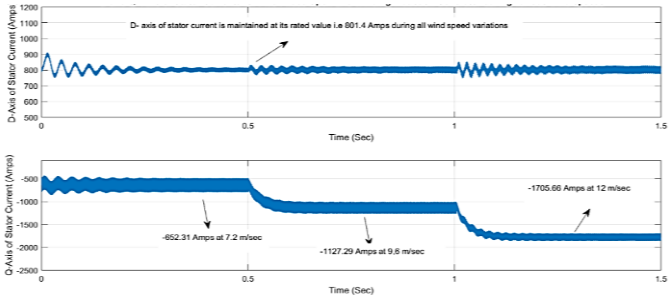

Figure 6. D and Q- axis stator Currents of Five Phase Open End Winding Squirrel Cage Induction Generator

Figure 6 illustrates that the d-axis of the stator current component remains consistently at its estimated value of 801.4Amps. However, the Q-axis of the stator current varies at different speeds: -652.31Amps at 7.2m/sec, -1127.29Amps at 9.6m/sec, -1705.66Amps at 12m/sec.

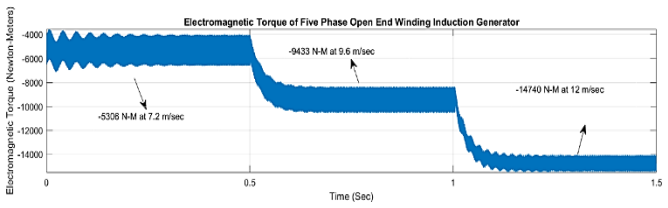

Figure 7. Electromagnetic Torque of Five Phase Open End Winding Squirrel Cage Induction Generator with two-level rectifier

Figure 7 illustrates that the Electromagnetic Torque of Five Phase Open End Winding Induction Generator with values -5306 N-M at 7.2m/sec, -9433 N-M at 9.6m/sec, -14740Amps at 12m/sec.

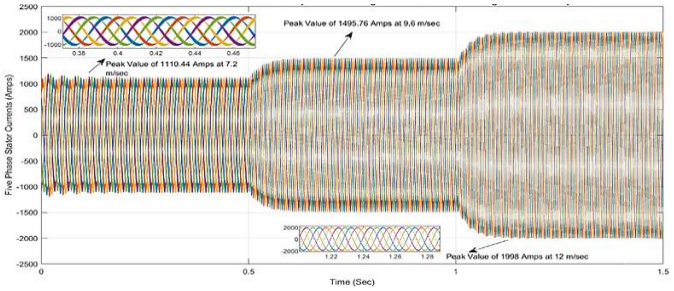

Figure 8. Five Phase Stator Currents of Five Phase Open End Winding Induction Generator with two-level rectifier

Figure 8 illustrates that the five phase stator currents of Five Phase Open End Winding Induction Generator with peak values of 1110.44 Amps at 7.2m/sec, 1495.76 Amps at 9.6m/sec, -1998Amps at 12m/sec.

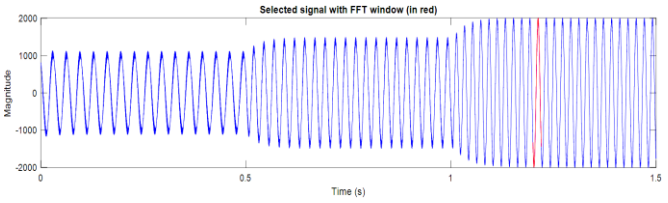

Figure 9. FFT Analysis of A- phase of stator current for Five Phase Open End Winding Squirrel Cage Induction Generator with two-level rectifier

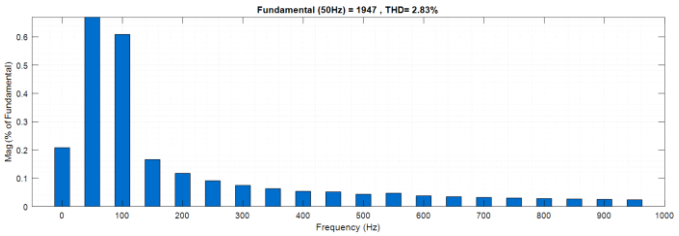

Figure 10. FFT Analysis of A- phase of stator current for Five Phase Open End Winding Squirrel Cage Induction Generator with two-level rectifier

From the *figures 9 and 10* it is observed that fundamental component of stator currents is 1947 Amps with a THD of 2.83 with two-level rectifier.

8. SIMULATION RESULTS OF FIVE PHASE OPEN END WINDING SQUIRREL CAGE INDUCTION GENERATOR USING IFOC TECHNIQUE WITH THREE LEVEL RECTIFIER

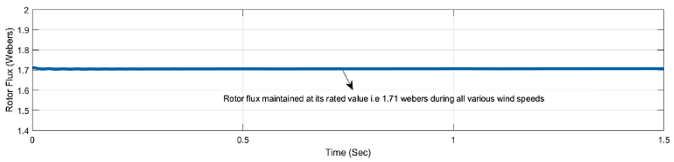

Figure 11. Rotor Flux of Five Phase Open End Winding Squirrel Cage Induction Generator

FOREX Publication
Open Access | Rapid and quality publishing
International Journal of Electrical and Electronics Research (IJEER)
Research Article | Volume 12, Issue 4 | Pages 1522-1530 | e-ISSN: 2347-470X

From *figure 12*, it is observed that rotor flux is maintained at its rated value 1.71 webers during all wind speed variations.

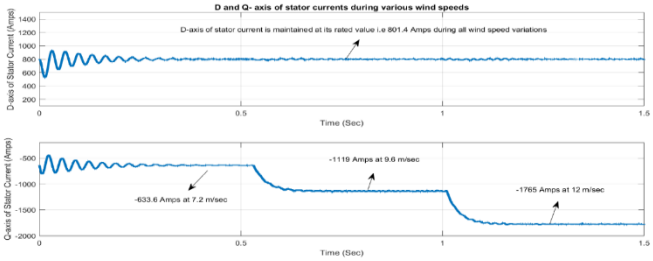

Figure 12. D axis and Q- axis stator currents of Five Phase Open End Winding Induction Generator with three-level rectifier

Figure 12 illustrates that the d-axis of the stator current component remains consistently at its estimated value of 801.4Amps. However, the Q-axis of the stator current varies at different speeds: -633.6Amps at 7.2m/sec, -1119Amps at 9.6m/sec, -1765Amps at 12m/sec.

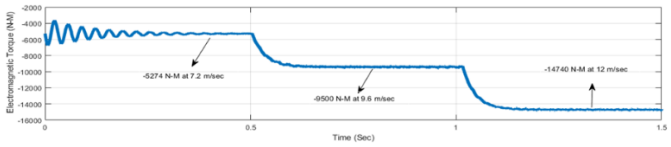

Figure 13. Electromagnetic Torque of Five Phase Open End Winding Induction Generator with three-level rectifier

Figure 13 illustrates that the Electromagnetic Torque of Five Phase Open End Winding Induction Generator with values -5310 N-M at 7.2m/sec, -9432.6 N-M at 9.6m/sec, -14740Amps at 12m/sec.

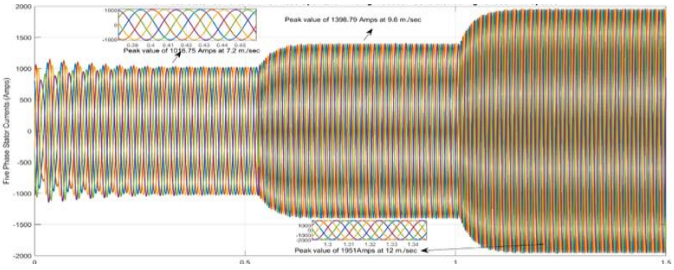

Figure 14. Five Phase Stator Currents of Five Phase Open End Winding Induction Generator with three-level rectifier

Figure 14 illustrates that the five phase stator currents of Five Phase Open End Winding Induction Generator with peak values of 1016.75 Amps at 7.2m/sec, 1398.79 Amps at 9.6m/sec, 1951Amps at 12m/sec.

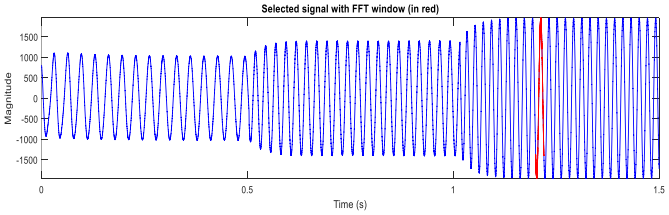

Figure 15. A- phase of stator current for Five Phase Open End Winding Induction Generator with three-level rectifier

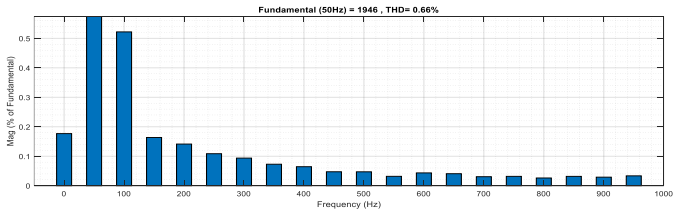

Figure 16. FFT Analysis of A- phase of stator current for Five Phase Open End Winding Induction Generator with three-level rectifier

From the *figures 15 and 16* it is observed that fundamental component of stator currents is 1947 Amps with a THD of 0.66 with three-level rectifier.

Table 1. Comparison Table for THD of stator currents using IFOC technique with Two Level and Three Level Rectifiers

Component	Fundamental component (Amps)	Total Harmonic Distortion (THD)%
Stator current of five phase open end winding induction generator using IFOC technique with two-level rectifier	1947	2.83%
Stator current of five phase open end winding induction generator using IFOC technique with three-level rectifier	1946	0.66%

Table.1 summarizes that THD component for stator current five phase open end winding induction generator (A-Phase) is reduced to 0.66% from 2.83 with three level rectifier which is better than two level rectifier with IFOC technique.

9. CONCLUSIONS

The application of Indirect Field Oriented Vector Control for five-phase open-end winding asynchronous generators in wind energy systems, particularly when integrated with three-level rectifiers, presents a significant advancement in renewable energy technology. By decoupling the control of torque and flux, Indirect Field Oriented Vector Control enables precise regulation of the generator's output, facilitating optimal energy extraction from wind resources across a range of speeds and load conditions. The harmonic currents of stator for five phase open end winding induction generator with three level rectifier is reduced drastically compared to two level rectifier.

REFERENCES

[1] Global Wind Energy Council, "Global Wind Report 2022," GWEC, Brussels, Belgium, 2022.

[2] I. G. Mason, S. C. Page, and A. G. Williamson, "A 100% renewable electricity generation system for New Zealand utilizing wind, geothermal, and hydro," Energy Policy, vol. 38, no. 8, pp. 3973-3984, Aug. 2010.

[3] J. G. McGowan and S. R. Connors, "Wind power: A turn of the century review," Annu. Rev. Energy Environ., vol. 25, no. 1, pp. 147-197, Nov. 2000.

[4] International Renewable Energy Agency (IRENA), "Renewable Power Generation Costs in 2020," IRENA, Abu Dhabi, UAE, 2021.

International Journal of Electrical and Electronics Research (IJEER)
Research Article | Volume 12, Issue 4 | Pages 1522-1530 | e-ISSN: 2347-470X

[5] J. Skea and S. N. J. Watson, "Renewable energy: Vision or reality?" Energy Policy, vol. 36, no. 12, pp. 4616-4620, Dec. 2008.

[6] A. G. Tindal, "Wind Energy and Economic Development," Renewable Energy World, vol. 24, no. 1, pp. 68-73, Jan. 2020.

[7] S. Heier, Grid Integration of Wind Energy Conversion Systems, 3rd ed. Hoboken, NJ, USA: Wiley, 2014.

[8] P. Rodriguez, A. Luna, R. Teodorescu, and F. Blaabjerg, "Grid synchronization of power converters using multiple second-order generalized integrators," IEEE Trans. Ind. Appl., vol. 53, no. 3, pp. 1938-1954, June 2008.

[9] S. Kouro, M. Malinowski, K. Gopakumar, J. Pou, L. G. Franquelo, and B. Wu, "Recent advances and industrial applications of multilevel converters," IEEE Trans. Ind. Electron., vol. 57, no. 8, pp. 2553-2580, Aug. 2010.

[10] R. H. Baker, "The role of squirrel cage induction generators in wind energy systems," Renewable Energy, vol. 36, no. 6, pp. 1677-1682, Jun. 2011.

[11] J. L. Rodriguez-Amenedo, S. Arnaltes, and J. C. Burgos, "Automatic generation control of a wind farm with variable speed wind turbines," IEEE Trans. Energy Convers., vol. 17, no. 2, pp. 279-284, Jun. 2002.

[12] P. Vas, Vector Control of AC Machines, 1st ed. Oxford, U.K.: Clarendon, 1990.

[13] H. Polinder, F. F. A. van der Pijl, G. J. de Vilder, and P. J. Tavner, "Comparison of direct-drive and geared generator concepts for wind turbines," IEEE Trans. Energy Convers., vol. 21, no. 3, pp. 725-733, Sep. 2006.

[14] E. Levi, "Multiphase electric machines for variable-speed applications," IEEE Trans. Ind. Electron., vol. 55, no. 5, pp. 1893-1909, May 2008.

[15] M. A. Abbas, T. O. Faiz, and M. El Moursi, "A review of fault-tolerant multiphase drive strategies for wind energy systems," Renewable Energy, vol. 137, pp. 31-42, Mar. 2019.

[16] A. Iqbal and E. Levi, "Multiphase machines for variable speed applications," Electric Power Components and Systems, vol. 36, no. 5, pp. 455-478, May 2008.

[17] N. Bianchi, S. Bolognani, and M. Zigliotto, "High performance control of a five-phase induction motor," IEEE Trans. Ind. Appl., vol. 36, no. 5, pp. 1334-1341, Sep. 2000.

[18] S. C. B. Ferreira, F. L. D. Silva, and R. A. G. Pereira, "Indirect field-oriented control of induction machines: A review," IEEE Trans. Ind. Electron., vol. 55, no. 5, pp. 2220-2231, May 2008.

[19] D. H. Lee, J. H. Park, and J. Y. Kim, "Design and implementation of an indirect field-oriented control for a squirrel-cage induction machine," IEEE Trans. Ind. Electron., vol. 56, no. 3, pp. 711-718, Mar. 2009.

[20] H. Abu-Rub, J. A. Gonzalez, and G. A. Capolino, Control of Electrical Drives, 2nd ed. Hoboken, NJ, USA: Wiley, 2014.

[21] A. Iqbal and E. Levi, "Control of induction machines with field-oriented techniques," Electric Power Components and Systems, vol. 36, no. 5, pp. 455-478, May 2008.

[22] M. A. L. Chinchilla, S. Arnaltes, and J. C. Burgos, "Control of permanent-magnet generators applied to variable-speed wind-energy systems connected to the grid," IEEE Trans. Energy Convers., vol. 21, no. 1, pp. 130-135, Mar. 2006.

[23] J. Rodriguez, J. S. Lai, and F. Z. Peng, "Multilevel inverters: A survey of topologies, controls, and applications," IEEE Trans. Ind. Electron., vol. 49, no. 4, pp. 724-738, Aug. 2002.

[24] J. Rodriguez, J. S. Lai, and F. Z. Peng, "Multilevel inverters: A survey of topologies, controls, and applications," IEEE Trans. Ind. Electron., vol. 49, no. 4, pp. 724-738, Aug. 2002.

[25] S. K. Sinha, "Analysis and control of multilevel inverters for wind energy systems," IEEE Trans. Energy Convers., vol. 24, no. 1, pp. 172-179, Mar. 2009.

[26] S. M. L. F. C. Almeida, J. A. C. de Azevedo, and M. A. M. de Lima, "Multilevel converters: A review of control strategies," Renewable and Sustainable Energy Reviews, vol. 16, no. 3, pp. 1640-1650, Apr. 2012.

[27] Bin Wu, Yongqiang Lang, Navid Zargari, and Samir Kouro "Power Converison and Control of Wind Energy Systems", ISBN: 9780470593653, July 2011.

[28] A. Iqbal, S. M. Ahmed, M. A. Khan, M. R. Khan and H. Abu-Rub, "Modeling, simulation and implementation of a five-phase induction motor drive system," 2010 Joint International Conference on Power Electronics, Drives and Energy Systems & 2010 Power India, New Delhi, India, 2010, pp. 1-6, doi: 10.1109/PEDES.2010.5712373.

© 2024 by the Swetha Kannepally, Ch. Murali, Mantri Srinivasarao, S Srikanth, and Adabala Ramakrishna. Submitted for possible open access publication under the terms and conditions of the Creative Commons Attribution (CC BY) license (http://creativecommons.org/licenses/by/4.0/).